

# Intrinsic Assessment Optimization Algorithm based Doubly Fed Induction Generator based Stability Analysis of Multi Machine System

V.Subha Seethalakshmi<sup>1</sup>, Dr. R. Karthigaivel<sup>2</sup>, N.Vengadachalam<sup>3</sup>, S.Selvakumaran<sup>4</sup>

<sup>1,3</sup>Assistant Professor, Department of EEE, TRP Engineering College, Trichy, Tamilnadu.

<sup>2,4</sup>Associate Professor, Department of EEE, P.S.N. College of Engineering and Technology, Dindigul, Tamil Nadu.

<sup>1</sup>vsubha05@gmail.com

**Abstract**-Over the past two decades, the rapid growth of the wind farm, based on the Doubly Field Induction Generator (DFIG) has been found. A DFIG based on this proposed work, introduced a power coordination technique designed for multi machine Offshore Wind Farm (OWF) and the power stability was further explored using the Intrinsic Assessment Optimization Algorithm (IAOA). Control and operation of both Grid Side Converter (GSC) and Rotor Side Converter (RSC) are analyzed. The RSC control loop monitors the maximum wind power and controls flux linkage. The GSC control loop maintains the stable DC voltage between the RSC and GSC and the DC connector voltage. The DFIG is connected in between the rotor terminals and utility grid via common dc link. The GSC is controlled by the DC bus and Alternative Current (AC) power circuits that allow the system to operate in a stable power supply system. An OWF is driven by the dual-power induction generator connected to an electrical network via a High-Voltage Direct Current (HVDC) link is presented for stability improvement using IAOA controller. The IAOA controller is used to provide full control of the offshore wind generation system. The IAOA controller is to effectively mitigate the problem of instability occurred in the offshore wind power generation system which shows the further impact on the stability of power generation in both RSC and GSC respectively. The performance of proposed IAOA strategy is validated through simulation based on Matlab Simulink software.

**Keywords:** Doubly Fed Induction Generator, Wind Power System, Stability Analysis, Intrinsic Assessment Optimization Algorithm (IAOA).

## 1. Introduction

In recent years, power systems have increased rapidly with a wind power reinforcement integration. Over the last two decade, the ratio of installed Wind Turbines (WTs) has increased and also the WTs costs has decreased. Recently installed windmills are variable speed wind turbines using mostly doubly fed induction generators. Many countries plan to build a number of large OWFs to

produce a large amount of sustainable and clean energy to meet their renewable energy goals. The functional block diagram of the DFIG based wind farm system is shown in Figure.1.

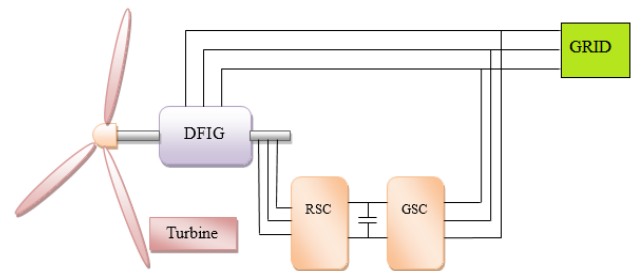


**Figure.1 Block Diagram of DFIG Based Wind Farm**

With the rapid growth of offshore wind energy installed capacity, the proportion of energy produced by OWF to that produced by conventional power plants has increased. Offshore wind farms with a capacity of several hundred MW are large enough to replace conventional power plants. The resulting power structure stability will be of great importance for large OWF effects. Furthermore, the well-known AC transmitting systems of the active operation of the VSC-HVDC transmission system are different in phase radiations.

Sometimes a wide variety of wind farms are integrated into a large-scale interconnected power system. Based on this situation, every wind farm systems are described with a corresponding DFIG. Total wind production can be considered as virtual wind plant that composes many equivalent DFIGs. An effective method is to reduce the order as an equivalent model. However, the equivalent model is usually calculated on a particular steady state error. Wind farms move to the unpredictability of the wind due to the changing and continuing state of the environment. Thus, the equivalent model is based on the same model as the stochastic; both structures and equivalent sample parameters are random.

In this paper, DFIG wind farms introduced an intrinsic assessment optimization algorithm with the equivalent sample architecture. The wind farm was clustered and compiled, and contains three

equivalent DFIGs of properties that describe various processes. The structure remained constant under various scenarios while the equivalent parameters changed. All historical scenes were coordinated and investigated. Each and every types of equivalent DFIG was classified into several groups according to their dynamic characteristics and was executed by utilizing representative DFIGs. Representative DFIG combinations have been made to produce all probable representative scenarios. Later, the Windmill farm representative had a simulator of displays and their Probability Distribution Function (PDF). Finally, the model was validated by simulations of the test system and the system depreciation rates under different scenarios were also studied.

## 2. Literature review

Several studies have been done demonstrating the ability to optimize wind configurations of renewable energy systems to maximize performance while minimizing cost. One of the most generally utilized stability techniques is the eigenvalue investigation dependent on state-space demonstrating. This technique has been connected to break down the stability of DFIG based wind farm power framework [1]. Numerous examinations have been improved unique exhibitions and transient stability of power frameworks through differential geometric and other correct linearization [2]. The reactive power control in ordinary working conditions and fault ride through ability amid fault conditions are both critical [3].

The normal for primary significance is inactivity. The higher the inactivity, the slower the rate of progress in rotor speed and stage edge, which diminishes the kinetic energy picked up amid fault [4]. The impact of Energy Storage System (ESS) on the power framework transient stability in a wind farm with Fixed Speed Induction Generator (FSIG), and the examination among DFIG and ESS-prepared FSIG from the flashing stability viewpoint [5]. The stability is evaluated utilizing potential and kinetic energies balance at a specific time. Energy work techniques have likewise considered in sustainable power source asset based controller structures [6]. At the point when a generator is an activity at specific restricts, a generator can expand the reactive creation power just by decreasing its creation of genuine power [7].

The most existing work, Sub Synchronous Resonance (SSR) was examined under deterministic working conditions, without thinking about the vulnerability of some essential elements, for example, the stochastic wind speed [8]. The starting point of these down to earth motions isn't yet obviously comprehended. In light of the recurrence secured,

these motions are viewed as random to Wind Turbine (WT) torsional communications [9]. Wind energy over the ocean surface can be used to produce vast electric power while maritime energy, for example, tidal, wave, marine momentum, and so on can likewise be adequately caught to deliver broad electric power sent to the power grid [10]. Its improvement influences numerous parts of power framework elements. In prior years the effects of incorporated DFIG on the electromechanical stability of common power frameworks have been wholly researched [11].

The Sub Synchronous Resonance (SSR) is where the wind farm convert energy with the dynamic framework to which it is associated, at least one characteristic frequencies of the electrical or mechanical piece of the entire power framework [12]. The effect on SSR from wind speed, remuneration degree, and control increases of the Rotor-Side Converter (RSC) is inspected [13]. The most well-known strategy is to sidestep RSC by utilizing the crowbar circuit, this technique is easy and straightforward, yet it results in DFIG losing its controllability and absorbing reactive power from the grid [14].

The rotor current controllers ought to be carefully tuned to guarantee closed-circle framework stability and satisfactory transient reaction inside the entire operational range [15]. The Voltage Source Inverter (VSI) gives the required polarizing current and control activity as a rule on the rotor side, and the rectifier is accountable for the primary power exchange by and large through the stator. The idea was started from the notable air conditioning DFIG utilized fundamentally in wind energy change frameworks [16]. A huge finding of the examinations demonstrates that the respectability of the structure following a recurrence occasion is conceivably traded off at immediately high infiltrations of wind [17].

Based on the second order model power angle of the dynamic characteristics is discussed. Accepting that the inherent possibilities of the synchronous generators are consistent, and the voltage extent variance has little exertion to active power [18]. At the point when the focal point of incorporation is to serve the expanding load request, the DFIG is explicitly included, and when the inside is on supplanting the old traditional age, the DFIGs are involved removing existing Synchronous Generator (SG) mostly or completely [19]. The capacity of wind turbines to give the recurrence bolster through the imitated dormancy, and additionally the possibilities for tuning such an appropriated reaction asset to guarantee a timely and compelling recurrence recuperation under various

framework conditions [20]. The symphonious voltages in the grid will cause harmonically distorted current output by the DFIG system, which will fall apart the power quality using Fuzzy logic control system [21]. A method has been developed in [22] for the operation analysis of self-excited induction generators (SEIGs) feeding battery charge loads via three-phase semi-converters by representing the battery circuit. In [23] the genetic algorithm technique has been applied twice in a nested loop for the design of three phase wind driven by self-excited asynchronous generators, using standard stator available and appropriate squirrel cage induction motor rotor frames. Genetic Algorithm (GA) tuned Integral and Propotional (IP) controller is proposed to design of decentralized Load Frequency Controller for interconnected thermal non-reheat power systems with AC-DC parallel tie-lines.

### 3. Materials and methods

The functional block diagram of proposed Intrinsic Assessment Optimization Algorithm (IAOA) based Multi machine DFIG system is shown in Figure 2. The proposed system consists of Grid Side Converter, Wind Generator and Rotor Side Converter. Based on the response of this converters the proposed system is to give active power on synchronous speed assortment to constant voltage and frequency. The magnitude and evolution of active power flows additionally controlled by utilizing RSC and GSC. The induction generator is associated with the wind turbine through a mechanical network comprise of high and low-speed shafts related with a gearbox.

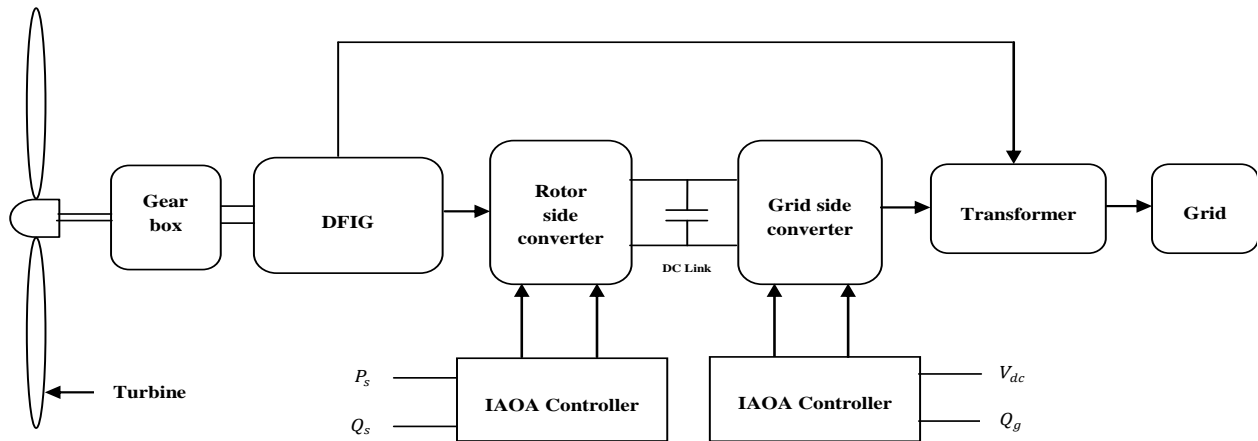


Figure.2 Basic Block Diagram of Proposed System

A diagram of the DFIG-based Windmill power unit, linked to a grid-coupled by a serial compensator transmission line is shown in Figure 2. The stator circuit of the DFIG is directly connected to the Point of Common Coupling (PCC). However, DFIG wind turbine system is interfaced with AC / DC / AC back-to-back PWM converter. The rotor side power electronic converter is used to control flow of power in both directions independently with real and reactive power. The machine implements both the super and the sub-synchronous speeds. The operation of the RSC will control the DFIG speed based on rotor current. The function of the GSC is to regulate the DC link voltage ( $V_{dc}$ ) by controlling the real power. It can be used for power factor control by controlling the reactive power.

#### 3.1. Wind generation model

The equivalent circuit if DFIG is shown in Figure 3. Depends upon the speed turn the energy of

the wind turbine is changed, the following equation (1) is used to validate the broadcasting flow of wind

$$W = \begin{cases} 0, S\partial \\ \frac{1}{2} \cdot \rho \cdot \pi \cdot P^2 \cdot U^3, S_d \leq S_\alpha \\ Qn \cdot S_{in} \leq U \propto \end{cases} \quad (1)$$

Where

$\partial$  = Air Flow

W = Wind Power

$S_{in}$  = Evaluated Speed of Wind

$S_d$  = Boot Speed of Wind

P = Farthest Point of the rotor

S = Speed of Wind

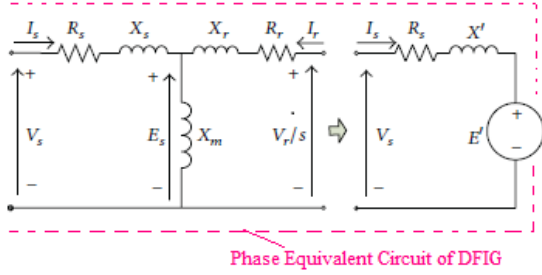


**Figure 3. DFIG – Phase equivalent circuit**

The Equation (2) is used to calculate the output power based on wind speed

$$w = \begin{cases} 0 & S(t) \leq S_{cut} - S_{in} \text{ or } S(t) \geq S_{cut} - S_{in} \\ Pr \frac{(S(t) - S_{cut} - S_{in})}{S_r - S_{cut} - S_{in}} & S_{cut} - S_{in} < S(t) < S_r \\ Pr & S_r < S(t) < S_{cut} - S_{out} \end{cases} \quad (2)$$

Where

S = Speed range of wind

Pr = Wind Turbine's rated power

$S_{cut} - S_{in}$ ,  $S_{cut} - S_{out}$  and  $S_r$  = Rated speed of the wind turbine

$PWT(t) = N_{wind} - PWT(t)$  is the general energy provided. The generator is demonstrated as a balanced voltage source in view of transitory impedance for balance examination. The active model of DFIG is appeared as

$$\frac{di_{qs}}{dt} = -\frac{w_{el}R_l}{w_s L_s} i_{qs} + w_{el} i_{ds} + \frac{w_{el}w_r}{w_s^2 L_s} e_{qs}^t - \frac{w_{el}}{T_r w_s^2 L_s} e_{qs}^t - \frac{w_{el}}{w_s L_s} v_{qs} + \frac{k_{mrr} w_{el}}{w_s L_s} v_{qr} \quad (3)$$

$$\frac{di_{ds}}{dt} = -w_{el} i_{qs} - \frac{w_{el}R_l}{w_s L_s} i_{ds} + \frac{w_{el}w_r}{w_s^2 L_s} e_{ds}^t - \frac{w_{el}}{T_r w_s^2 L_s} e_{ds}^t - \frac{w_{el}}{w_s L_s} v_{ds} + \frac{k_{mrr} w_{el}}{w_s L_s} v_{dr} \quad (4)$$

$$\frac{d^v_{qs}}{dt} = w_{el} R_2 i_{ds} - \frac{w_{el}}{T_r w_s} e_{qs}^t + w_{el} \left( \frac{w_s - w_r}{w_s} \right) e_{ds}^t - K_{mr} w_{el} v_{dr}$$

$$\frac{d^v_{ds}}{dt} = -w_{el} R_2 i_{ds} - \frac{w_{el}}{T_r w_s} e_{ds}^t + w_{el} \left( \frac{w_s - w_r}{w_s} \right) e_{qs}^t + K_{mr} w_{el} v_{qr} \quad (5)$$

Where

$d^v_{qs}$  = Q axis Voltage

$d^e_{ds}$  = d axis Voltage

$i_{ds}$  = stator current of d-axis

$i_{qs}$  = stator current q-axis

### 3.2. Rotor side converter

The RSC can control the DFIG speed and flux through the control of the rotor flows. This control is practiced in the dq reference frame to maintain a strategic distance from time-shifting inductances in the DFIG model. Alignment of the axis-d with the rotor flux vector forming an angle of  $\theta_{\phi_r}$  with the axis  $\alpha$  and rotating with the control angular velocity  $w_{\phi_r}$  provides decoupled between the electromagnetic torque and the supply of rotor flux. Figure 4 demonstrates the schematic diagram for the rotor control system. Applying the RSC in the same reference frame as the DFIG, as is simulated, avoids the transformation of quantities between different reference frames and makes the system more convenient for control.

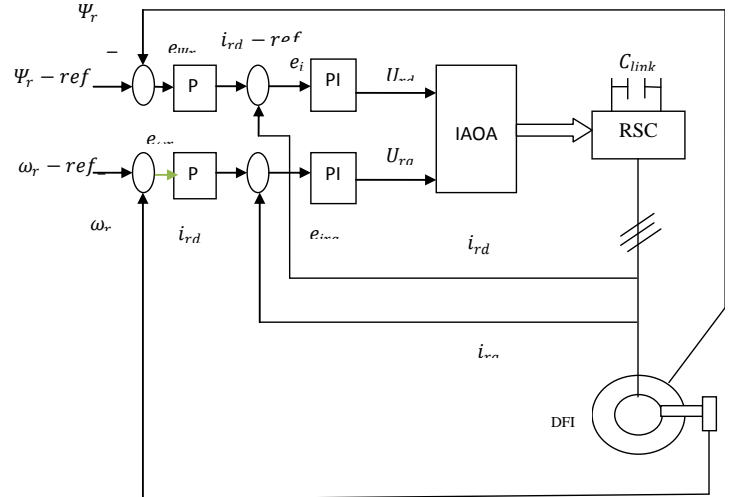


**Figure 4. Schematic Diagram of RSC**

Assigning the speed and rotor flux reference values, the PI control of reference turbine is used to generate the rotor current vector.

$$i_{rd} - ref = \left( K_{p\phi_r} + \frac{K_{I\phi_r}}{s} \right) e_{\phi_r} \quad (6)$$

$$i_{rd} - ref = \left( K_{p\omega_r} + \frac{K_{I\omega_r}}{s} \right) e_{\omega_r} \quad (7)$$

Where

$K_{p\phi_r}$  and  $K_{I\phi_r}$  = Gain of speed

$K_{p\omega_r}$  and  $K_{I\omega_r}$  = Gain of Flux

$e_{\phi_r}$  = Error Rate of Rotor Speed

$e_{\omega_r}$  = Error Rate of Rotor Flux.

The error value of present PI controller is calculated based on the difference value of reference current and rotor current.

$$u_{rd} = \left( K_{pir} + \frac{K_{Iir}}{s} \right) e_{ird} \quad (8)$$

$$u_{rq} = \left( K_{pir} + \frac{K_{Iir}}{s} \right) e_{irq} \quad (9)$$

$K_{pir}$  and  $K_{Iir}$  = Gain Response of Rotor Current

$e_{ird}$  and  $e_{irq}$  = Error Rate of Rotor Current.

The reference voltage is generated and fed to DFIG's rotor using control loops of rotor ( $u_{rd}, u_{rq}$ ). The rotor flux reference frame is used to run the RSC and DFIG, the output of the current controller has been straightly connected to rotor with no change.

### 3.3. Grid side converter

Active power of Grid Side Converter is controlled by using DC voltage regulation (Vdc), while the quadrature axis current is used to regulate the input power factor, which uses the immediate axis current to accurately control the DC connector voltage. The higher harmonic content is reduced in grid using line filter  $L_g, R_g$ . The mathematical expression of  $u_{gcd}$  and  $u_{gcq}$  in terms of  $i_{gd}, i_{gq}, u_{sd1}, u_{sq1}$  and  $\omega_1$  are used to generate the d and q axis current in GSC.

$$u_{gcd} = R_g i_{gd} + L_g \frac{d}{dt} i_{gd} - \omega_1 L_g i_{gq} + \frac{1}{N_2} \left( \frac{\sqrt{3}}{2} u_{sd1} + \frac{1}{2} u_{sq1} \right) \quad (10)$$

$$u_{gcq} = R_g i_{gq} + L_g \frac{d}{dt} i_{gq} - \omega_1 L_g i_{gd} + \frac{1}{N_2} \left( \frac{\sqrt{3}}{2} u_{sq1} + \frac{1}{2} u_{sd1} \right) \quad (11)$$

Figure 5 shows the schematic diagram of the GSC control. This control conspire empowers the free control of  $i_{gd}$  and  $i_{gq}$  through  $i_{gd-ref}$  and  $i_{gq-ref}$ .

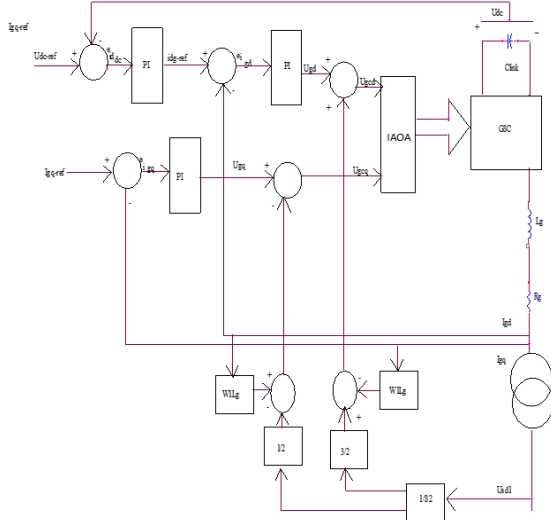


**Figure.5. Grid Side Converter**

The  $u_{sd1}$  and  $u_{sq1}$  are feed forward terms, such are expressed as  $u_{sd}$  and  $u_{sq}$

$$u_{sd1} = u_{sd} \cos(\theta_{us} - \theta_{\varphi r}) + u_{sd} \sin(\theta_{us} - \theta_{\varphi r}) \quad (12)$$

$$u_{sq1} = -u_{sd} \sin(\theta_{us} - \theta_{\varphi r}) + u_{sd} \cos(\theta_{us} - \theta_{\varphi r}) \quad (13)$$

Since the stator voltage in the reference frame is zero equivalent to the Q axis part, the

following mathematical expression is defined as the reference frame angles.

$$\theta_{us} - \theta_{\varphi r} = \arctan\left(\frac{u_{sq}}{u_{sd}}\right) \quad (14)$$

$$u'_{gd} = R_g i_{gd} + L_g \frac{d}{dt} i_{gd} \quad (15)$$

$$u'_{gq} = R_g i_{gq} + L_g \frac{d}{dt} i_{gq} \quad (16)$$

By substituting mathematical equations (14) to (16) to get the dq axis value of grid side converter and expressed as equation (17) and (18).

$$u_{gcd} = u'_{gd} - \omega_1 L_g i_{gq} + \frac{1}{N_2} \sqrt{\frac{3}{2}} u_{sd1} \quad (17)$$

$$u_{gcq} = u'_{gq} - \omega_1 L_g i_{gd} + \frac{1}{N_2} \frac{1}{2} \sqrt{\frac{3}{2}} u_{sd1} \quad (18)$$

### 3.4. INTRINSIC ASSESSMENT OPTIMIZATION ALGORITHM

Intrinsic optimization evaluation is a kind of method that tracks the control signal at the output of the reference model response. It presents the advantages of simple structure and stable and fast reconfiguration. The general idea is to incorporate a reference model that underlies the acquisition of preferred closed-loop reactions. IAQA designs the mechanism law and adjustments technique to drive the desired trajectories for the system to track the reference model output. The schematic diagram of IAQA is shown figure 6.

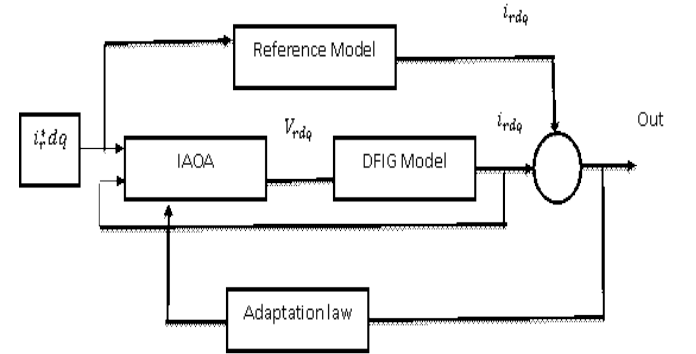


**Figure 6. Model Diagram of Intrinsic Assessment Optimization**

In this work can specify the first-order model given the rotor current control output of the turbine system:

$$\frac{di_{rd}}{dt} = -a \cdot i_{rd} + b \cdot V_{rd}^r \quad (19)$$

$$\frac{di_{rq}}{dt} = -a \cdot i_{rq} + b \cdot V_{rq}^r \quad (20)$$

Where  $i_{rd}$  and  $i_{rq}$  is the system state, a and b are the system model parameters,  $V_{rd}^r$  is the control signal.

$$V_{rd}^r = k(t) \cdot i_{rdq} + kr(t) \cdot i_{rdq} \quad (21)$$

Where:  $i_{rdq}$  is the reference signal,  $k(t)$  and  $kr(t)$  are the feedback and the feed forward gain respectively. For controlling the system, the outputs of rotor current controller may be rewritten as follows

$$\frac{di_{rdqm}}{dt} = a \cdot i_{rdqm} + b_m \cdot i_{rdq} \quad (22)$$

Where  $i_{rdqm}$  is the state of the reference model,  $a_m$  and  $a_m$  are the reference model parameters and the algorithm steps are discussed below

**Step 1:** Generate primary particles by using random velocity and position.

**Step 2:** Set controller parameters, and calculate the velocity fitness function.

$$v_{i,max} = \frac{x_{i,max} - x_{i,min}}{N} \quad (23)$$

$$v_{i,min} = -v_{i,max}$$

Where,

$x_{i,max}$ , and  $x_{i,min}$  = upper and lower bond of the particles

$v_{i,max}$  and  $v_{i,min}$  = maximum and minimum of velocity

**Step 3:** If all particles have been set, go to the next step. Otherwise, go to the second step.

**Step 4:** Generate new particles by updating the velocity.

$$\text{If } v_{i,j}(t+1) > v_{j,max} \text{ then } v_{i,j}(t+1) = v_{j,max}$$

$$\text{If } v_{i,j}(t+1) < v_{j,min} \text{ then } v_{i,j}(t+1) = v_{j,min}$$

$$V_{i,j} = \text{Input variables of velocity}$$

**Step 5:** Generate new particles by updating the position

$$\text{If } x_{i,j}(t+1) > x_{j,max} \text{ then } x_{i,j}(t+1) = x_{j,max}$$

$$\text{If } x_{i,j}(t+1) < x_{j,min} \text{ then } x_{i,j}(t+1) = x_{j,min}$$

$$x_{i,j} = \text{Input variables of position}$$

**Step 6:** If the stopping criteria are satisfied, go to the next level. Otherwise, go to the second step.

**Step 7:** Analysis the output values.

**Step 8:** stop the process.

The process have been entered several times to reach an average network. During the verification process, both the RSC and GSC regions will be further identified using the Controlled pulses to Switches in the topology.

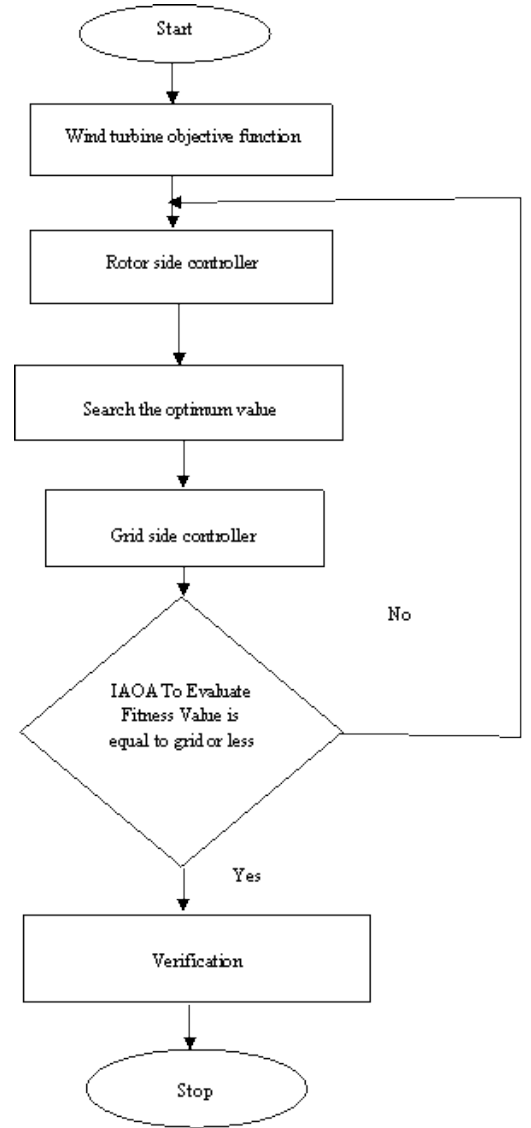


**Figure.7 Flowchart of IAOA**

**Figure.7** shows the flowchart that describes the operating stages for the DFIG system. At the initial step, the system read the input data and optimizes the problem using the Intrinsic Assessment Optimization Algorithm (IAOA), and it refers both input and output and provides the practical result in the overall system and the following parameters are used to validate the performance of proposed system.

#### Peak Time

The response is to reach the peak value in the starting time is called peak time, it is denoted by  $t_p$ . The derivative of the response is zero.

$$t_p = \frac{\pi}{w_d} \quad (24)$$

Where,

$$t_p = \text{peak time}$$

$$w_d = \text{damped frequency}$$

#### Peak overshoot

Peak overshoot is also known as maximum overshoot, and it is defined as the deviation of the peak time response from the final value of the response.

$$m_p = c(t_p) - c(\infty) \quad (25)$$

Where,

$m_p$  = peak overshoot

$c(t_p)$  = peak value of the response

$c(\infty)$  = steady state value of the response

### Steady State Error

The steady-state error can occur because of nonlinearities in our system, but this is beyond our scope. Consider error that arises because of the system itself and its input.

Steady state error is the difference between the source and the reference voltage of the system, and the time goes to the infinity, it will depend on the type of the input signal line (step, ramp and parabolic input).

$$\text{Steady State Error} = \frac{\text{Reference Voltage}}{\text{Source Voltage}} \quad (26)$$

In this system, the error is considered in the variations of the reference voltage and the source voltage. The efficiency of IAOA based DFIG system is evaluated by using following mathematical expression.

$$\beta = \frac{P_{out}}{P_{in}} \quad (27)$$

$P_{in}$  of DFIG can be understood by fast currents and voltages, as indicated by the accompanying condition.

$$P_{in} = i_a V_a + i_b V_b + i_c V_c \quad (28)$$

$P_{out}$  is controlled by the torque evaluation of the shaft and the rotor speed takes after.

$$P_{out} = T_{shaft} * w_r \quad (29)$$

The following equation is used to evaluate the Efficiency of proposed system.

$$\beta = \frac{T_{shaft} * w_r}{i_a V_a + i_b V_b + i_c V_c} \quad (30)$$

## 4. Results and discussion

In this section discuss the proposed windmill system to analyze the results of simulation and performance. MATLAB2017a is used to develop the simulator model of the proposed multi-machine system is shown in Figure.8

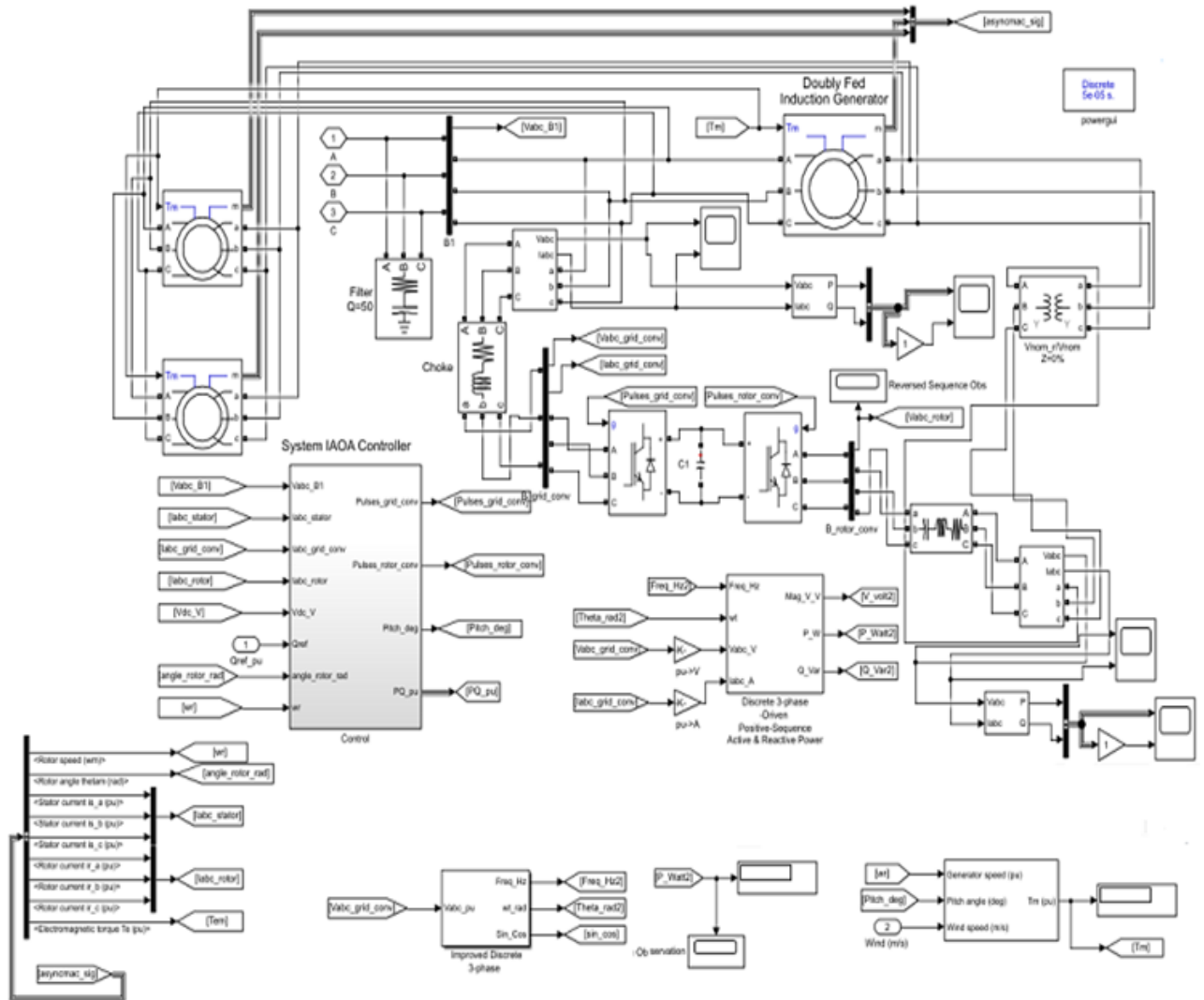


Figure 8. Proposed simulation – Simulink Model

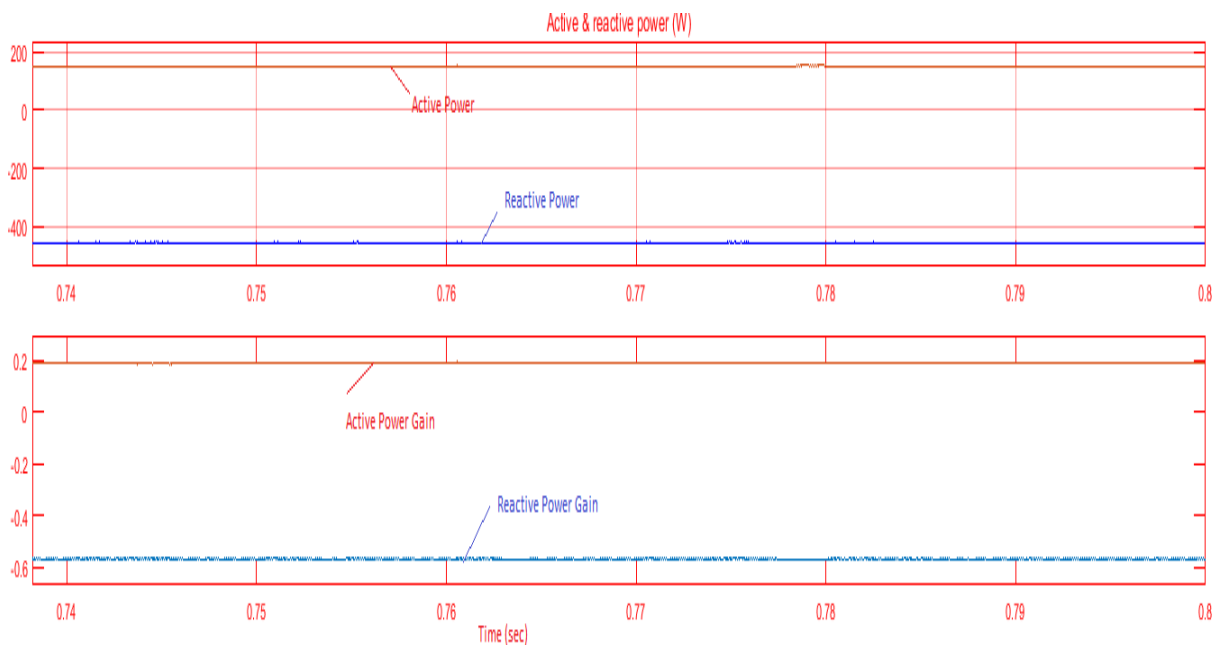
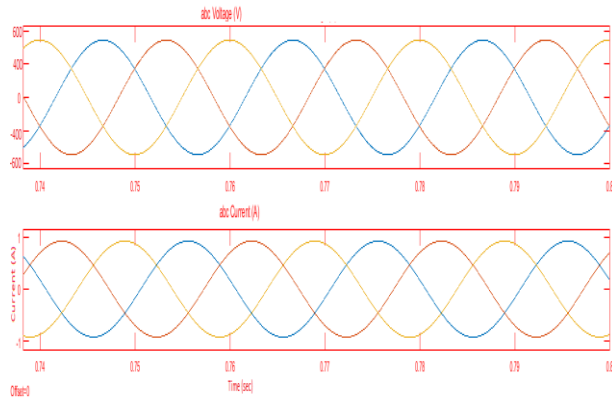


Figure 9. Power and Gain response of Grid

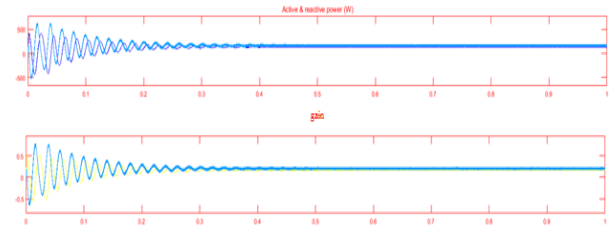


Figure 9 shows the active and reactive power and gain response of grid system. A DFIG controller for an appropriate and beneficial change of energy is fundamental and unavoidable. The power has magnitudes in relation to the grid-side converter, such as reactive power and active power near their optimum values.



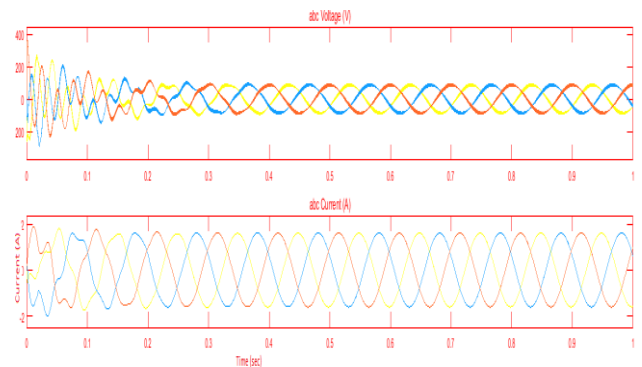
**Figure 10. Grid voltage Grid current**

The above figure 10 shows the voltage and current response of grid. By using IAOA method the grid side converter is given the perfect result for every working condition. Because the performances on reference tracking and disturbance rejection has sufficiently optimized with proposed IAOA design procedure.



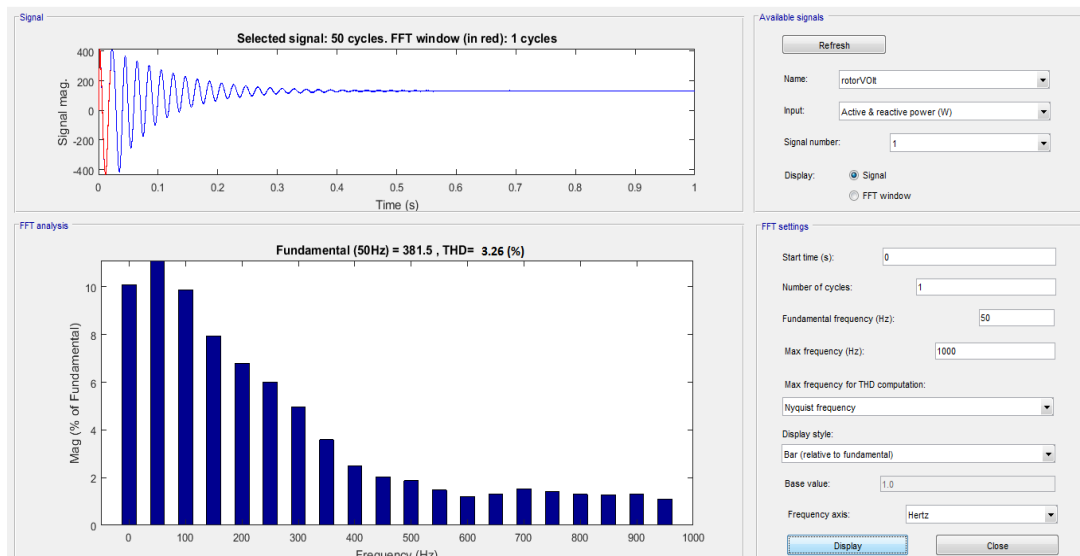
**Figure 11. Rotor Power Response and Gain**

Figure 11 shows the active and reactive power and the gain of the rotor system. The proposed method can easily track the reference signal of the active and reactive power of a dynamic system. In this response, power control is verified that the proposed method is robust in the performance of the conventional method.



**Figure 12. Rotor Voltage and Rotor Current**

The proposed IAOA based Rotor Voltage and Rotor Current response was appeared in figure 12. By using IAOA method the rotor converter is given the perfect result because reference tracking and disturbance rejection has sufficiently optimized with proposed IAOA design procedure.



**Figure 13: THD analysis of Rotor side converter Voltage**

The THD analysis of Rotor side converter is shown in Figure 13 using IAOA method. By using

IAOA method to achieve low THD equivalent to 3.26% and a major component at 50Hz.

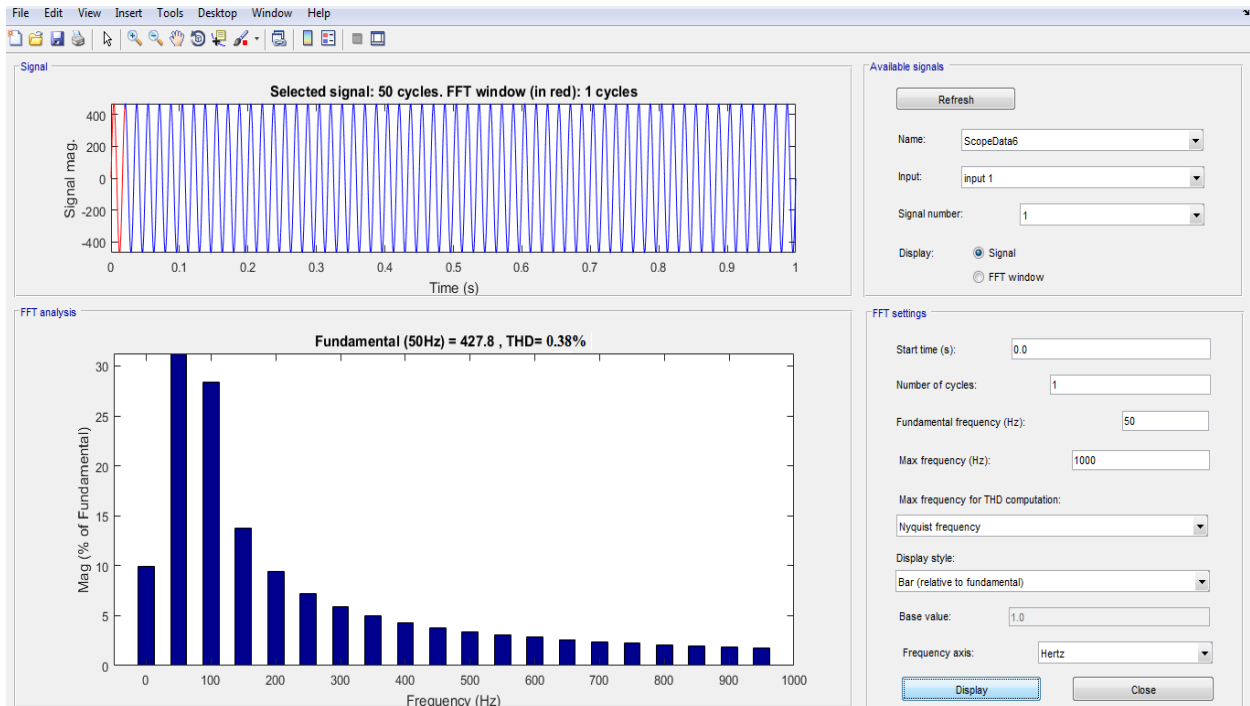


Figure 14. THD analysis of grid side converter Voltage

Figure 14 shows the THD analysis of the proposed system in grid side converter and it is essential to monitor the input voltage in grid line and output power to the inverter side of the system, in this system produce Total Harmonics Distortion is 0.38% by using IAOA method.

Table.1 Comparison analysis of THD

Method	Direct Fuzzy	STOA	Proposed IAOA
Power Source	Wind	Wind	Wind
Output power per unit	0.8	0.85	0.9
THD Rotor Side (%)	4.89	4.02	3.26
THD Grid Side (%)	4.57	3.99	0.38

Table.1 shows the comparative analysis of the THD value and output power comparison in the existing Direct Fuzzy, Substantial Transformative Optimization Algorithm (STOA) with IAOA system. As compared with existing method the proposed method give the perfect result.

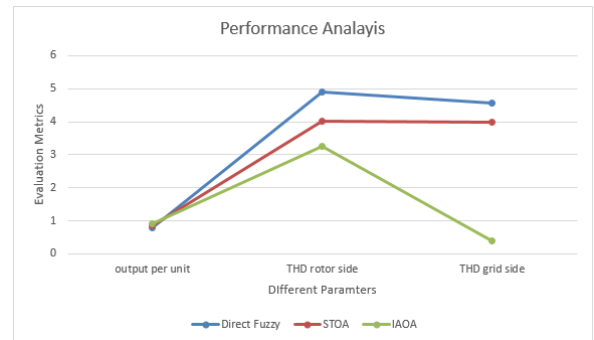


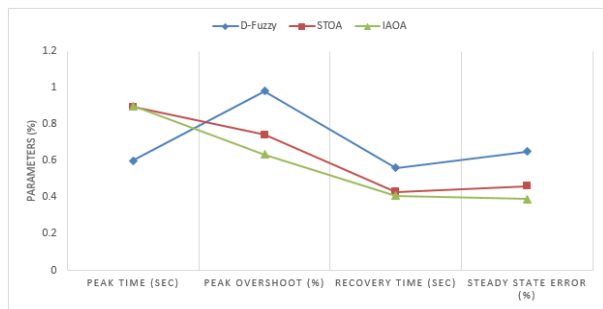
Figure 15. Comparison Chart

Figure.15 shows the comparison of output power and THD response in the proposed IAOA system with existing Direct Fuzzy (D-Fuzzy), STOA. As compared with existing methods the proposed method give very low level THD response.

Table.2 Control system parameters

Method	Direct Fuzzy	STOA	Proposed IAOA
Peak Time (sec)	0.6002	0.8948	0.9012
Peak Overshoot (%)	0.9814	0.7414	0.6341
Recovery Time (sec)	0.56	0.43	0.41
Steady State Error (%)	0.65	0.46	0.39

Table.2 shows the control system parameters comparison is peak time, peak overshoot, recovery time, and the steady-state error of this system.



**Figure 16. Comparison Chart of Control System Parameters**

Figure.16 shows the table comparing the control system load parameters such as peak time, peak overshoot, recovery time and steady state errors in the existing system with the proposed method. Compared to existing methods of the proposed method IAOA give perfect results against all parameters.

## 5. Conclusion

In this paper, the modeling and control of a Doubly Fed Induction Generator based on multi-wind turbine-generator system was considered. More precisely, the modeling of the different components, the control strategies for the back-to-back converter have been studied and analyzed in detail. IAOA is implemented in the wind turbine system, which carry, the GSC control, the pitch angle control LRC control and a maximum power point tracking control, respectively. The objective of the control vector system for the network-side converter controller is used to maintain the constant voltage across the capacitor and produce a unity power factor operation of the grid. Domain time analysis based on simulation results is performed. By using IAOA method the THD result of 3.26% in rotor side converter and 0.38% in grid side converter are achieved.

## References

1. Yunyang. Xu & Heng Nian, "Frequency Coupling Characteristics Modeling and Stability Analysis of Doubly Fed Induction Generator", IEEE Transactions on Energy Conversion, vol.33 ,no.3, pp.1475-1486,2018.
2. Boyu Qin & Xuemin Zhang, "Input to state stability based control of doubly fed induction generator", IEEE Transactions on Power Systems , vol.33,no.3, pp.2949-2961,2018.
3. Che-Hao Chang & Bing-Lin Kuan, "Stability Improvement of a Two Area Power System Connected with an Integrated onshore and offshore Wind system Using a STATCOM", IEEE Transactions on Industry Applications ,vol.53,no.2, pp.867-877 ,2017.
4. Jie Ying & Xiaoming Yuan, "Inertia Characteristics of DFIG based WT under Transient Control and Its Impact on the First Swing Stability of SGs", IEEE Transactions on Energy Conversion, Vol.32, no.4 , pp.1502-1511 ,2017.
5. Saeed Afsharnia & AzinAslani, "A Study on Power System's Transient Stability in Determination of the Appropriate Generator Type for Wind Turbines: Comparison between fixed-speed induction generator equipped with energy storage system and doubly-fed induction generator", 10th International Conference on Environment and Electrical Engineering, Rome ,Italy , pp.1-4,2011.
6. Reza Yousefian, & RojanBhattarai, "Transient Stability Enhancement of Power Grid with Integrated Wide-Area Control of Wind Farms and Synchronous Generators", IEEE Transactions on Power Systems, vol.32,no.6, pp.4818-4831,2017.
7. Nguyen HuuHieu & Le Hong Lam, "Using Double Fed Induction Generator To Enhance Voltage Stability And Solving Economic Issue", 2016 IEEE International Conference on Sustainable Energy Technologies (ICSET), Hanoi, Vietnam , pp.374-378 ,2016.
8. Wuhui Chen & Xiaorong Xie, "Probabilistic Stability Analysis of Subsynchronous Resonance for Series Compensated DFIG based Wind Farms" , IEEE Transactions on Sustainable Energy, vol.9 ,no.1, pp.400-409,2018.
9. Dong Wang & Liang Liang , "Analysis of Low-Frequency Stability in Grid-Tied DFIGs by Non-Minimum Phase Zero Identification", IEEE Transactions on Energy Conversion, vol.33, no.2, pp.716-729,2017.
10. Li Wang & Chun Yu Lin, "Stability Analysis of a Microgrid System With a Hybrid Offshore Wind and Ocean Energy Farm Fed to a Power Grid through an HVDC Link", IEEE Transactions on Industry Applications, vol.54,no.3, pp.2012-2022,2018.
11. Jiabing Hu & Hao Yuan, "Modeling of DFIG-Based WTs for Small-Signal Stability Analysis in DVC Timescale in Power Electronized Power Systems", IEEE Transactions on Energy Conversion,vol.32,no.3, pp.1151-1165,2017.
12. M. A. Chowdhury, "SSR Mitigation of Series-Compensated DFIG Wind Farms by a

- Nonlinear Damping Controller Using Partial Feedback Linearization”, IEEE Transactions on Power Systems, vol.33, no.3, pp.2528-2538,2018.
13. Huakun Liu & Chuanyu Zhang, “Quantitative SSR Analysis of Series- Compensated DFIG-Based Wind Farms using Aggregated RLC Circuit Model”, IEEE Transactions on Power Systems, vol.32,no.1, pp.474-483,2017.
  14. Donghai Zhu & Xudong Zou, “Feed forward Current References Control for DFIG Based Wind Turbine to Improve Transient Control Performance During Grid Faults”, IEEE Transactions on Energy Conversion, vol. .33 , no.2 , pp.670-681,2018.
  15. Michael K. Bourdoulis & Antonio T. Alexandridis , “Direct Power Control of DFIG Wind Systems Based on Nonlinear Modeling and Analysis” IEEE journal of emerging and selected topics in power electronics, vol.2 ,no.4 , pp.764-775,2014.
  16. Sergio M. A. Cruz & Gil D. Marques, “Predictive Torque and rotor Flux Control of a DFIG-dc System for Torque-Ripple Compensation and Loss Minimization”, IEEE Transactions on industrial electronics, vol.65,no.12, pp.9301-9310,2018.
  17. Shuo Wang & Jiabing Hu, “Virtual Synchronous Control for Grid-Connected DFIG-based Wind Turbines”, IEEE Journal of Emerging in Power Electronics, vol.3 ,no.4, pp.932-944,2018.
  18. ZihuaNiu & Gengyin Li , “Analysis of Doubly Fed Induction Generator Dynamic Action to Power Angle Oscillation”, IEEE PES Asia-Pacific Power and Energy Engineering Conference (APPEEC), Kowloon ,china & pp.1-5,2013.
  19. Abhilash Kumar Gupta & KusumVerma, “Impact analysis of DFIG location on low-frequency oscillations in power system”, The 6th International Conference on Renewable Power Generation, p.1413-1417,2017.
  20. Abdelhak Dida & Djilani Ben Attous, “Doubly-fed induction generator drive based WECS using fuzzy logic controller”, Frontiers in Energy , vol.9 ,no.3, pp.272-281,2017.
  21. Mohamed M.Ismail Ahmed & F.Bendary, “Protection of DFIG wind turbine using fuzzy logic control” Alexandria Engineering Journal,vol.55,no.2 , pp.941-949,2013.
  22. R Karthigaivel, N Kumaresan, M Subbiah ,”Analysis and control of self-excited induction generator-converter systems for battery charging applications”,IET Electric Power Applications, vol. 5, no.2, pp.247-257,2013.
  23. R Karthigaivel, N Kumaresan, P Raja, M Subbiah, “A novel unified approach for the analysis and design of wind-driven SEIGs using nested Gas”, Wind engineering, vol. 33, no.6, pp.631-647.
  24. S Selvakumaran, V Rajasekaran, R Karthigaivel “Genetic algorithm tuned IP Controller for load frequency control of interconnected power systems with HVDC links”, Archives of Electrical Engineering, vol.63, no.2, pp.161-175,2018.